

# Do critical Casimir forces induce colloidal phase transitions in a near-critical solvent ?

John R. Edison,<sup>1</sup> Nikos Tasios,<sup>1</sup> Simone Belli,<sup>2</sup> Robert Evans,<sup>3</sup> René van Roij,<sup>2</sup> and Marjolein Dijkstra<sup>1,\*</sup>

<sup>1</sup>*Soft Condensed Matter, Utrecht University,  
Princetonplein 5, 3584 CC Utrecht, The Netherlands*

<sup>2</sup>*Institute for Theoretical Physics, Utrecht University,  
Leuvenlaan 4, 3584 CE Utrecht, The Netherlands*

<sup>3</sup>*H.H. Wills Physics Laboratory, University of Bristol, Bristol BS8 1TL, United Kingdom*

## Abstract

In 1978 Fisher and de Gennes predicted the existence of long-ranged solvent-mediated (SM) interactions between two colloidal particles suspended in a near-critical binary solvent. The range of these (universal) SM forces, often referred to as critical Casimir forces, is set by the correlation length of the solvent which diverges on approaching its critical point. The remarkable sensitivity of these particular SM interactions to the temperature and composition of the solvent sparked recent interest, driven by prospects of unparalleled control of colloidal self-assembly in a tunable, reversible, and in-situ fashion. Here we determine both the effective SM pair interactions and the *full* phase diagram of Brownian discs suspended in an explicit two-dimensional *supercritical* binary liquid mixture. We find colloidal gas-liquid and fluid-solid transitions in a surprisingly large regime *away* from the critical point of the solvent reservoir. We argue that critical Casimir interactions, defined for a pair of colloids, cannot account for these transitions; *many-body* SM interactions are required. Our simulation study, supported by a mean-field theory, provides a fresh perspective on colloidal self-assembly mediated by solvent critical fluctuations, and opens new avenues for controlling and manipulating this process.

---

\* m.dijkstra1@uu.nl

Colloidal particles dispersed in a binary solvent mixture have an inherent preference for one of the two solvent species. This is reflected by preferential adsorption of the favoured species on the colloid surface, leading to the development of adsorbed films. Such films can mediate an effective interaction between two colloidal particles which is remarkably sensitive to the thermodynamic state of the solvent. Close to the (demixing) critical point of the solvent the adsorbed film thickness is determined by the correlation length  $\xi$  of the solvent [1] and, as first predicted by Fisher and de Gennes [2], the resulting solvent-mediated (SM) interactions are long-ranged, with universal scaling properties. An analogy between the confinement of quantum fluctuations of the electromagnetic field [3] and that of thermal composition fluctuations in a near-critical binary solvent led to these (universal) SM forces being referred to as critical Casimir forces. Theoretical studies on near-critical fluids confined between a pair of infinitely large planar walls (representing two static large colloids) [4–8], along with direct experimental measurements of the Casimir force [9, 10] between a colloid and a wall have advanced our understanding of the nature of two-body SM interactions. However, the phase behaviour of a *dense* suspension of colloids is largely unexplored, due to the geometrical complexity and the high-dimensional parameter space; these demand massive computational costs. Here we seek to understand the strength and range of the SM interactions and the resulting phase behaviour of a dense colloidal suspension as a function of the thermodynamic state of the solvent via computer simulations. The conventional approach of treating the solvent implicitly via an effective two-body colloidal pair interaction is likely to fail as the SM interactions are expected to be highly non-additive when the correlation length is of the same size as the colloidal particles.

However, computer simulation of colloids in an explicit molecular solvent with a bulk correlation length that diverges upon approaching the critical point is notoriously difficult as very different length and time scales are involved. Nevertheless, by sacrificing one spatial dimension and using a lattice model, we have been able to calculate the SM interactions and *full* phase diagrams for a ternary solvent-solvent-colloid mixture, thereby revealing phenomena not captured by treatments based *solely* on effective pair potentials extracted from the *static* planar slit system [11].

We model the ternary solvent-solvent-colloid mixture as an incompressible ABC mixture on a 2D square lattice, as shown schematically in Fig. 1. Colloids C are discretized hard discs with a radius of  $R$  lattice sites, occupying a fraction  $\eta$  of the lattice sites. Every site

that is left unoccupied by the colloidal discs is occupied by either a solvent molecule of species A or B, such that the fraction of sites occupied by A and B equals  $1 - \eta - x$  and  $x$ , respectively. We consider only nearest neighbour AB repulsions and BC attractions: an energy penalty  $\frac{1}{2}\epsilon > 0$  is assigned to every nearest neighbour AB pair to drive AB demixing at sufficiently low temperatures  $T$ , and an energy gain  $-\frac{1}{2}\alpha\epsilon$  with  $\alpha \geq 0$  for every BC pair to mimic the colloid C's preference for species B. Throughout we set the lattice spacing to unity.

In the limit  $\eta = 0$ , our model reduces to a binary AB mixture that is isomorphic to the 2D lattice (Ising) model, the workhorse in studies on critical phenomena and inhomogeneous fluids for the last four decades. The critical temperature of this binary mixture is  $T_c = 0.567\epsilon/k_B$ , and its thermodynamic state is characterized fully by the reduced temperature  $\tau = (T - T_c)/T_c$  together with either the reduced chemical potential difference  $\Delta\mu_s = (\mu_B - \mu_A)/\epsilon$  between species B and A or the composition  $x$ . For  $\Delta\mu_s < 0$  the AB mixture favours an A-rich composition at all temperatures. Moreover for  $\tau < 0$  demixing into an A-rich state ( $x < 0.5$ ) and a B-rich state ( $x > 0.5$ ) takes place at  $\Delta\mu_s = 0$ , with a critical point  $\{\tau_c = 0, x_c = 0.5\}$ , see Fig. 2a and b. In the two limits  $\Delta\mu_s \rightarrow \pm\infty$  our ABC mixture reduces to the 2D AC or BC hard-disc system with packing fraction  $\eta$  in an (irrelevant) pure A solvent ( $x = 0$ ) or pure B solvent ( $x = 1 - \eta$ ). Barring small discretization and lattice artifacts, and ignoring subtleties regarding the (non-)existence of a stable hexatic phase, these AC and BC systems exhibit fluid-solid coexistence for  $\eta \in [0.700, 0.716]$  as represented by vertical dashed lines in Fig. 3a-c [12].

Throughout this work we study colloids immersed in a *supercritical* (one-phase) AB mixture, relatively poor in the colloid-preferred species B ( $\eta > 0, \tau > 0$ , and  $\Delta\mu_s \leq 0$ ). This choice precludes solvent-mediated colloidal aggregation arising from complete wetting and capillary condensation [13]. The solvent is treated grand canonically, i.e. we view our system as being in thermal and diffusive contact with an AB solvent reservoir with composition  $x_r$  that fixes  $\tau$  and  $\Delta\mu_s$ . We treat the colloidal suspension at given  $\eta$  in osmotic equilibrium with this reservoir. The ABC mixture has composition  $x \neq x_r$ . Note that the variable  $\tau$  merely sets the temperature, and is not a measure of distance from criticality of the ternary mixture. We consider first the case of neutral colloids of radius  $R = 6$ , which have no preference for species A or B ( $\alpha = 0$ ) [14], illustrated in Fig. 2c and in SI-movie-01 where we show a system of these colloids (right) at  $\tau = 0.005$  and  $\Delta\mu_s = 0$  in equilibrium with the solvent

reservoir (left). The snapshots reveal the tendency of the colloids to preferentially adsorb at the ‘interfaces’ between the instantaneous (*supercritical*) A and B domains. This feature, which resembles the binding of colloids to static air-liquid or liquid-liquid interfaces by a Pieranski potential [15], is captured here owing to the Brownian character of the colloids. Fig. 2d and SI-movie-02 show results for the same parameter set, except now the colloids strongly prefer solvent B ( $\alpha = 19$ ). The strong B-adsorption on the colloids and the unfavourable AB interaction lead to an overall excess of B, thereby driving the ABC mixture far away from criticality; the solvent correlation length is observed to be much smaller than the particle size.

In the remainder of this study we focus on the case  $\alpha = 0.6$  where B-rich layers adsorbed on the colloid surfaces compete with a supercritical A-rich bulk solvent ( $\tau > 0$  and  $\Delta\mu_s < 0$ ). In Figs. 3a and b we present the phase diagram of the ternary mixture in the  $\Delta\mu_s$  vs  $\eta$  representation at three reduced temperatures  $\tau = 0.025, 0.05, 0.075$ . The correlation length of the AB solvent reservoir at the isochoric composition ( $\Delta\mu_s = 0, x_r = 0.5$ ) is given by  $\xi = 0.567/\tau$ , and for these temperatures:  $\xi_{0.025} = 22.68$ ,  $\xi_{0.05} = 11.35$ ,  $\xi_{0.075} = 7.56$ , which are of the same order as the size of the colloid  $R = 6$ . Although the underlying AB solvent reservoir is supercritical, our simulations reveal that a non-zero concentration of large Brownian discs induces stable colloidal gas (G), liquid (L), and crystal (X) phases as well as two-phase G-L and G-X coexistence. The G-L coexistence, shown more clearly in Fig. 3b, terminates at a critical point that shifts to lower  $\Delta\mu_s$  and higher  $\eta$  with increasing  $\tau$ . Tracing the locus of the three critical points of the ABC mixture from  $\tau = 0.075$  through 0.05 to 0.025, it appears that the critical points of the colloidal G-L transition are continuously connected to the critical point of the binary solvent mixture ( $\eta = \tau = \Delta\mu_s = 0$ ); investigations at smaller  $\tau$  are constrained by our computational resources.

For  $\Delta\mu_s < -0.1$  we also observe G-X coexistence with a broad colloid density gap that narrows sharply upon lowering  $\Delta\mu_s$ , consistent with the limiting hard-disc fluid-solid coexistence at  $\Delta\mu_s \rightarrow -\infty$  (vertical dashed lines). Significantly, this decreasing density gap at G-X coexistence suggests an additional underlying metastable G-L lower critical point. Although we have not been able to identify this in our MC simulations, such an additional critical point does occur in our mean-field theory presented below. Moreover, if we accept hard-disc coexistence in the opposite limit  $\Delta\mu_s \rightarrow \infty$ , then we also expect a G-L-X triple point at  $\Delta\mu_s \simeq -0.06$  for  $\tau = 0.025$  (see Fig. 3b), and at even lower  $\Delta\mu_s$  for higher  $\tau$ .

In Figs. 3d - 3f and in SI-movie-03/04/05 we show results for systems of  $256 \times 512$  lattice sites simulated at reduced temperature  $\tau = 0.05$  ( $\alpha = 0.6, R = 6$ ) that illustrate configurations of (d) a supercritical (homogeneous single-phase) fluid state, (e) G-L coexistence, and (f) G-X coexistence. In all three cases the local solvent composition is strongly correlated with the local colloid density, such that the coexisting L phase in (e) and X phase in (f) have a binary BC composition with tiny traces of A. Conversely in the coexisting G phases shown in Figs. 3e and 3f the solvent composition is very close to the composition of the reservoir  $x \simeq x_r$ . In Fig. 3c we convert the phase diagram of Fig. 3a into the  $x_r - \eta$  representation. It is evident from the snapshots and Figs. 3c and 2b that for all observed G-L and G-X coexistence: (i) the composition of the solvent reservoir  $x_r < 0.2$  is far from its critical composition  $x_c = 0.5$ , and (ii) the correlation length of the solvent is smaller than the colloid radius,  $\xi < R$ . Strikingly, in the homogeneous supercritical state of Fig. 3d the correlation length (the typical size of the A-rich and BC-rich "patches") is clearly much larger than the colloid radius and thus far exceeds that of the solvent reservoir. This reflects the nearby (G-L) critical point of the ternary mixture which, as noted previously, appears to be continuously connected to the critical point of the binary AB solvent mixture ( $\eta = \tau = \Delta\mu_s = 0$ ). In fluid mixtures where the species interact via short range potentials, all structural correlations decay with the same correlation length [16]. Therefore along the G-L critical locus, solvent-solvent, colloid-colloid and solvent-colloid correlations should decay with the same, diverging correlation length. We have confirmed this numerically by calculating the BB, BC and CC pair correlation functions; see Fig. S2 of the supplementary information (SI). We have also confirmed the divergence of the long wavelength limit of the structure factor  $S_{BB}$  upon approaching the critical point of the ternary mixture at a fixed value of temperature  $\tau = 0.025$ ; see Fig. S3 of the SI.

As mentioned earlier, there have been several attempts to ascertain the phase behaviour of colloids in a near-critical solvent based solely on effective two-body interactions, e.g. [11, 17]. In order to assess the validity of this approach for the present system we calculated several one- and two-colloid properties for the range of thermodynamic state points studied above. For the three temperatures investigated we show in Fig. 4 the dependence on  $\Delta\mu_s$  of (a) the thickness  $\lambda$  of the adsorbed B-rich film on a single disc, (b) the minimum  $U_{min}$  of the effective pair potential  $U(r) = -k_B T \log[P(r)/P(\infty)]$ , where  $P(r)$  is the probability of finding two colloids separated by a center-of-mass distance  $r$ , obtained from the transition

matrix Monte Carlo method, (see Methods) and (c) the reduced second virial coefficient  $B_2^* = \int_0^\infty (1 - \exp[-U(r)/k_B T]) r dr / 2R^2$ , normalized to that of 2D hard discs. For convenience, we also show in Fig. 4d the phase diagrams in the  $\eta$ - $\Delta\mu_s$  representation. The film thickness  $\lambda$  and the well depth  $U_{min}$  are measures of the range and strength of  $U(r)$ , respectively. The quantity  $B_2^*$  is a well-established (dimensionless) measure of combined strength and range that must be sufficiently negative in order for gas-to-liquid condensation to occur in systems described by pairwise additive interactions [18, 19]. Fig. 4a shows a monotonic increase of the film thickness from  $\lambda \ll R$  to  $\lambda \gg R$ , reflecting the growth of the correlation length, as the isochoric composition is approached ( $\Delta\mu_s \rightarrow 0$ ). In the same range the strength  $U_{min}$  varies non-monotonically being strongest at slightly negative  $\Delta\mu_s$ , reaffirming earlier theoretical predictions [20, 21].

At  $\Delta\mu_s \simeq 0$  the effective pair potential  $U(r)$  is long-ranged, however it is only *weakly* attractive ( $U_{min}/k_B T < 1$ ). Upon further decreasing  $\Delta\mu_s$ ,  $U(r)$  does become more attractive, although the adsorbed film thickness  $\lambda$  (and thereby the range of  $U(r)$ ) decreases.  $B_2^*$  also becomes more negative. Upon lowering  $\Delta\mu_s$  further the range and strength of  $U(r)$  becomes smaller and weaker respectively, such that  $B_2^*$  increases and even becomes positive, indicative of a predominant repulsive pair force. Given the information obtained from  $B_2^*$  and  $U(r)$  one can attempt to draw conclusions about the phase diagram, an actual estimation of which is shown in Figs. 3a) and 4d). Although the observation of G-L coexistence in the region between  $-0.05 < \Delta\mu_s < 0$  might be consistent with the two-body description, the observed triple point and G-X co-existence for  $\Delta\mu_s < -0.05$ , are not. In other words, in this regime the phase diagram of the full ABC mixture reflects the importance of non-pairwise effective SM interactions. Our simulation results clearly indicate that the usual paradigm of employing only effective pair potentials as obtained from e.g. planar slit studies and the Derjaguin approximation simply breaks down when it comes to describing the full phase diagram of the ternary mixture.

In analogy with colloid-polymer mixtures, the narrowing of the G-X phase boundaries (see Fig. 3a) and the short range of the SM interactions (see Fig. 4a), upon lowering  $\Delta\mu_s$ , strongly suggests the existence of an underlying metastable G-L critical point. Within a mean-field approximation we analyzed the Helmholtz free energy associated with the Hamiltonian of our ABC model (see Methods section). In Fig. 5, we plot the resulting phase diagrams for various  $\tau > 0$ , which reveal a closed-loop immiscibility gap and *two* G-L

critical points. We show a three-dimensional representation in Fig. S1 of the SI. The upper critical point approaches smoothly the critical point of the colloid-free AB solvent mixture as  $\tau \rightarrow 0$ . Interestingly, we find that the immiscibility gap shrinks with increasing  $\tau$  until the two critical points merge and disappear at  $\tau \simeq 0.09$ . We also observe coexistence of two crystal phases with the same (hexagonal) symmetry but different lattice spacings, also terminating at a critical point (the 'cusp' at the lower right corner of Fig. 5). The *topology* of the mean-field phase diagram and its  $\tau$ -dependence are remarkably consistent with that obtained from simulations.

The phase behaviour of colloids in a near-critical solvent is rich; we observe (i) G-L and G-X coexistence, (ii) the G-L and G-X coexistence occur far from the critical point of the solvent reservoir and the locus of G-L critical points appears to connect smoothly to it and (iii) many-body interactions are crucial to account for the observed colloidal phase behaviour. While neutral colloids suspended in a near-critical solvent ( $\Delta\mu_s \simeq 0$ ) sit at the 'interface' of the fluctuating domains, colloids preferring a certain solvent species drag in that species, thereby shifting the ternary system away from criticality.

It is evident that the topology of the phase diagram of colloidal particles in a near-critical binary solvent stems from an intricate balance between competing colloid-solvent and solvent-solvent couplings that can only be captured in a treatment of the full ternary mixture. The picture that emerges is that the resulting many-body SM interactions between the colloids will drive colloidal G-L and G-X phase transitions with a strong accompanying solvent demixing, but only when the correlation length of the solvent reservoir is of the order of the colloidal size or smaller. This begs the question whether (universal) critical Casimir interactions, defined for a pair of colloids, can induce colloidal phase transitions [17]. Our results also question whether these pairwise interactions can account for the mechanism behind colloidal aggregation reported in recent experimental work [22].

We speculate that the topology of the phase diagrams we present is likely to hold for an analogous 3D system (hard sphere colloids) as there is nothing particular to two dimensions. Given that we find broad phase coexistence well-removed from the critical point of the solvent, experiments for reversibly manipulating and controlling self-assembly processes and colloidal nanoparticles in solvent mixtures should be less demanding than previous studies would suggest. In addition, our study might yield new insight into recent experiments and simulations that suggest that two dimensional plasma membranes of living cells induce

long-range critical Casimir interactions between proteins[23, 24].

## Model and simulations

Our model is based on that of Rabani *et al.* [25]. We model the colloidal suspension as an incompressible ABC mixture on a 2D square lattice. Colloids C are discretized hard discs (HD) with a radius of  $R$  lattice sites that can undergo translational motion on the square lattice. The hard-disc Hamiltonian  $H_C$  is zero for non-overlapping configurations, and infinite if any pair of colloids overlap. Every lattice site  $i$  has an occupancy number  $n_i = 1$  if it is occupied by a colloidal disc, and 0 if it is available for an A or a B solvent molecule. For sites with  $n_i = 0$  we associate an occupancy number  $s_i = -1$  if the site is occupied by A, and  $s_i = 1$  if by B. We consider only nearest neighbour interactions and assign an energy penalty  $\epsilon/2 > 0$  for every nearest neighbour AB pair to drive AB demixing at sufficiently low temperatures and an energy gain of  $-\alpha\epsilon/2$  with  $\alpha \geq 0$  for every BC pair to mimic preferential adsorption of solvent B on the colloid surfaces. The total Hamiltonian thus reads

$$H = H_C + \frac{\epsilon}{4} \sum_{\langle i,j \rangle} (1 - s_i s_j)(1 - n_i)(1 - n_j) - \frac{\alpha\epsilon}{4} \sum_{\langle i,j \rangle} n_i(1 + s_j)(1 - n_j) \quad (1)$$

where the summation runs over the set of distinct nearest neighbour pairs  $ij$ . We performed simulations in an elongated simulation box of  $256 \times 512$  sites for three different values of the reduced temperature  $\tau = 0.025, 0.05$ , and  $0.075$ . At each  $\tau$  we performed simulations in the  $(\eta, \tau, \Delta\mu_s)$ -ensemble. For packing fractions  $\eta$  of hard discs that lie within the binodal curve, we can observe two-phase coexistence in the simulation box. The packing fractions of the coexisting phases can be obtained from the resulting density profiles of the hard discs. In order to determine the G-L coexistence more accurately we treat the colloids grand canonically using the staged-insertion technique [26] in combination with the transition matrix (TM) MC method, see e.g.[26–28]. We also utilise the TMMC technique to measure the probability  $P(r)$  of finding two colloids, suspended in a near-critical solvent at a certain  $\Delta\mu_s$  and  $\tau$ , to be separated by a distance  $r$ .

## Mean-field expression for the Helmholtz free energy

Within a mean-field theory the Helmholtz free energy (per lattice site) of the incompressible ABC mixture can be decomposed as  $F = F_C + F_{AB} + U_{BC}$ , with (i) the pure-colloid contribution  $F_C(\eta, T)$  (ii) the mean-field free energy  $F_{AB}(x, \eta, T)$  of the binary AB mixture in the free space in between the colloids (with fractions  $1 - x'$  and  $x' \equiv x/(1 - \eta)$  of A and B, respectively), and (iii) the average adsorption energy  $U_{BC}$  of the B solvent on the colloid surfaces. This yields, up to irrelevant constants,

$$F(\eta, T, x) = F_C(\eta, T) + \frac{2\epsilon x(1 - x - \eta)}{(1 - \eta)} + k_B T \left[ x \ln \frac{x}{1 - \eta} + (1 - x - \eta) \ln \left( \frac{1 - x - \eta}{1 - \eta} \right) \right] - \frac{Z\alpha\epsilon}{v_c} \frac{x\eta}{1 - \eta} \quad (2)$$



where  $Z \simeq 2\pi R$  is the effective colloidal coordination number and where  $v_c \simeq \pi R^2$  is the effective volume (area in 2D) of the colloid. For  $F_C(\eta, T)$  we employ the hard-disc free energy from Ref. [29] for the fluid phase, and from Ref. [30] for the solid phase. (More details of the theory will be presented in a future paper.) The phase diagram shown in Fig. 5 is based on  $Z\alpha = 32$  and  $v_c = 1000$ , which do not correspond to values used in our simulation studies. We do not attempt to make a quantitative comparison between the results of our mean field approach and those of simulations, rather we attempt to understand the simulation phase diagrams *qualitatively* and investigate the possibility of a lower (metastable) G-L critical point.

- 
- [1] Flöter, G & Dietrich, S. (1995) *Z. Phys. B* **97**, 213–232.
  - [2] Fisher, M. E & de Gennes, P. G. (1978) *C. R. Acad. Sci. Paris B* **287**, 207–209.
  - [3] Casimir, H. B. G. (1948) *Kon. Ned. Akad. Wetensch. Proc.* **51**, 793.
  - [4] Krech, M. (1994) *The Casimir Effect in Critical Systems*. (World Scientific, Singapore).
  - [5] Evans, R & Stecki, J. (1994) *Phys. Rev. B* **49**, 8842–8851.
  - [6] Hanke, A, Schlesener, F, Eisenriegler, E, & Dietrich, S. (1998) *Phys. Rev. Lett.* **81**, 1885–1888.
  - [7] Krech, M. (1999) *J. Phys. Condens. Matter* **11**, R391.
  - [8] Vasilyev, O, Gambassi, A, Maciolek, A, & Dietrich, S. (2009) *Phys. Rev. E* **79**, 041142.
  - [9] Hertlein, C, Helden, L, Gambassi, A, Dietrich, S, & Bechinger, C. (2008) *Nature* **451**, 172–5.
  - [10] Gambassi, A, Maciolek, A, Hertlein, C, Nellen, U, Helden, L, Bechinger, C, & Dietrich, S. (2009) *Phys. Rev. E* **80**, 061143.
  - [11] Mohry, T. F, Maciolek, A, & Dietrich, S. (2012) *J. Chem. Phys.* **136**, 224902.
  - [12] Bernard, E. P & Krauth, W. (2011) *Phys. Rev. Lett.* **107**, 155704.
  - [13] Evans, R. (1990) *J. Phys. Condens. Matter* **2**, 8989–9007.
  - [14] Pandit, R, Schick, M, & Wortis, M. (1982) *Phys. Rev. B* **26**, 5112.
  - [15] Pieranski, P. (1980) *Phys. Rev. Lett.* **45**, 569–572.
  - [16] Evans, R, Leote de Carvalho, R. J. F, Henderson, J. R, & Hoyle, D. C. (1994) *J. Chem. Phys.* **100**, 591–603.
  - [17] Nguyen, V. D, Faber, S, Hu, Z, Wegdam, G. H, & Schall, P. (2013) *Nat Commun* **4**, 1584.
  - [18] Noro, M. G & Frenkel, D. (2000) *J. Chem. Phys.* **113**, 2941–2944.
  - [19] Vliegthart, G. A & Lekkerkerker, H. N. W. (2000) *J. Chem. Phys.* **112**, 5364–5369.
  - [20] Drzewiński, A, Maciolek, A, & Evans, R. (2000) *Phys. Rev. Lett.* **85**, 3079–82.

- [21] Okamoto, R & Onuki, A. (2012) *J. Chem. Phys.* **136**, 114704.
- [22] Bonn, D, Otwinowski, J, Sacanna, S, Guo, H, Wegdam, G, & Schall, P. (2009) *Phys. Rev. Lett.* **103**, 156101.
- [23] Veatch, S. L, Cicuta, P, Sengupta, P, Honerkamp-Smith, A, Holowka, D, & Baird, B. (2008) *ACS Chemical Biology* **3**, 287–293.
- [24] Machta, B. B, Veatch, S. L, & Sethna, J. P. (2012) *Phys. Rev. Lett.* **109**, 138101.
- [25] Rabani, E, Reichman, D. R, Geissler, P. L, & Brus, L. E. (2003) *Nature* **426**, 271–274.
- [26] Ashton, D. J & Wilding, N. B. (2011) *Mol. Phys.* **109**, 999–1007.
- [27] Errington, J. R. (2003) *Phys. Rev. E* **67**, 012102.
- [28] Escobedo, F. A. (2007) *J. Chem. Phys.* **127**, 174104.
- [29] Santos, A, López de Haro, M, & Bravo Yuste, S. (1995) *J. Chem. Phys.* **103**, 4622.
- [30] Young, D. A & Alder, B. J. (1979) *J. Chem. Phys.* **70**, 473–481.

## ACKNOWLEDGMENTS

We thank N. Wilding, D. Ashton and A. Maciolek for stimulating discussions. J.R.E. and M.D. acknowledge financial support from a Nederlandse Organisatie voor Wetenschappelijk Onderzoek (NWO) VICI grant. N.T. and M.D. acknowledge financial support from an NWO-ECHO grant. J.R.E., N.T. and M.D. acknowledge a NWO-EW grant for computing time in the Dutch supercomputer Cartesius. R.E. acknowledges financial support from the Leverhulme Trust.

**Author contributions:** J.R.E. and M.D. initiated the simulation part of the project. N.T. and J.R.E. performed the simulations and were supervised by M.D.. S.B. and J.R.E. worked on the theory and were supervised by R.v.R.. J.R.E., N.T., S.B., R.E., R.v.R., and M.D. co-wrote the paper. All authors analyzed and discussed results.

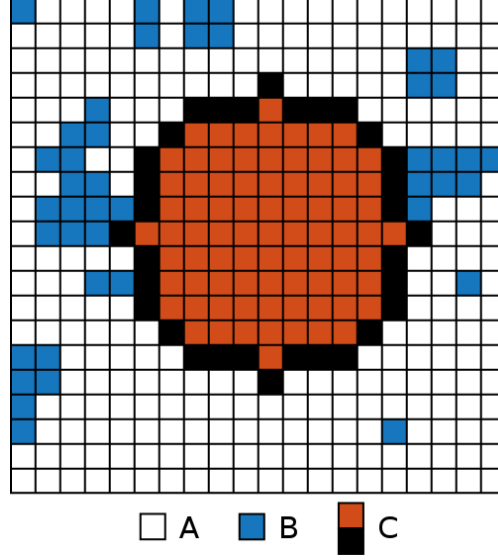


FIG. 1. **A schematic representation of the solvent-solvent-colloid lattice model.** White cells are occupied by solvent species A, blue cells by solvent species B, and brown and black cells represent the interior and the boundary of a single colloidal particle C, respectively. Nearest neighbour AB pairs experience a repulsive potential  $\epsilon/2$ , and nearest neighbour BC pairs an attractive potential  $-\alpha\epsilon/2$ .

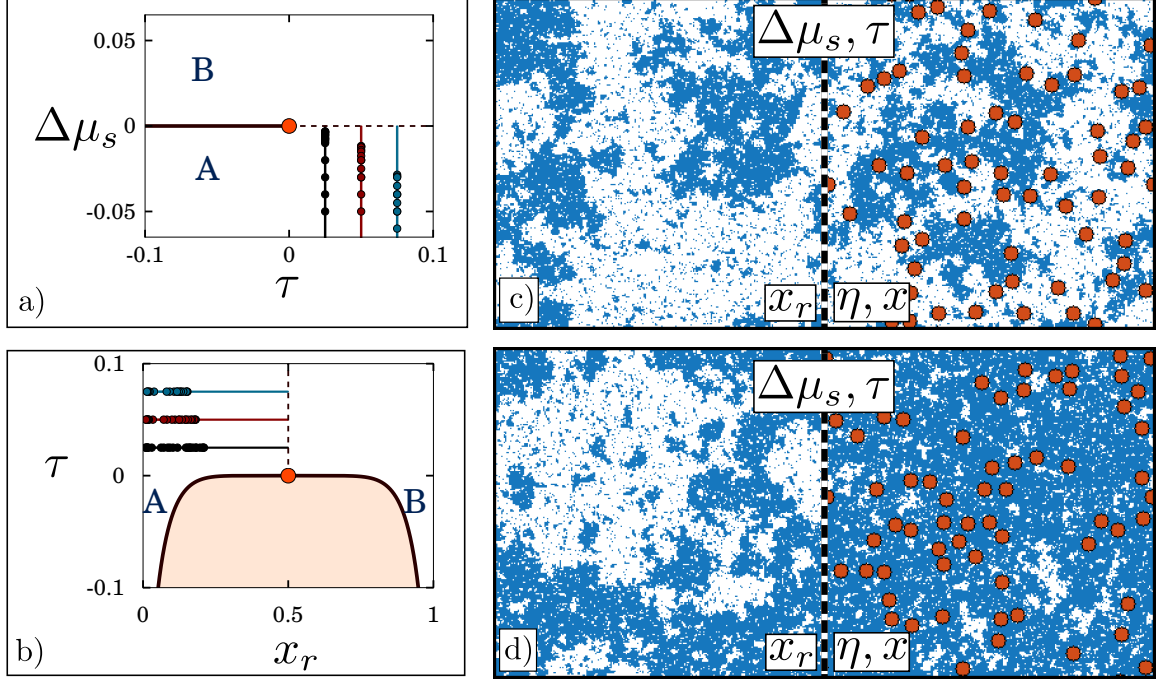


FIG. 2. **Ternary ABC solvent-solvent-colloid mixture** : a) Phase diagram of the colloid-free AB solvent mixture plotted as  $\Delta\mu_s$  vs  $\tau$ . b) Phase diagram (binodal) of the same mixture plotted as  $\tau$  vs  $x_r$ , the composition of the solvent. The two coexisting phases for  $\tau < 0$  are designated A and B. In a) and b) the lines correspond to the paths along which the phase diagram of the full ternary ABC mixture is determined; the dots represent the states where phase coexistence is observed and the orange dot indicates the critical point of the AB solvent mixture ( $\tau = 0$ ,  $\Delta\mu_s = 0$ ). c) Typical configurations of a ternary ABC mixture (right) with neutral colloids with no preference for A or B (radius  $R = 6$ ,  $\alpha = 0$ ) at colloid packing fraction  $\eta = 0.11$  and solvent composition  $x = (1 - \eta)/2$  in equilibrium with a solvent reservoir (left) with  $\eta = 0$ ,  $x_r = 1/2$ ,  $\tau = 0.005$ , and bulk correlation length  $\xi \approx 19R$ . d) Typical configurations of a ternary ABC mixture (right) with colloids strongly preferring solvent B ( $R = 6$ ,  $\alpha = 19.0$ ) at packing fraction  $\eta = 0.11$  and solvent composition  $x > (1 - \eta)/2$  in equilibrium with the same solvent reservoir (left) as in (c).

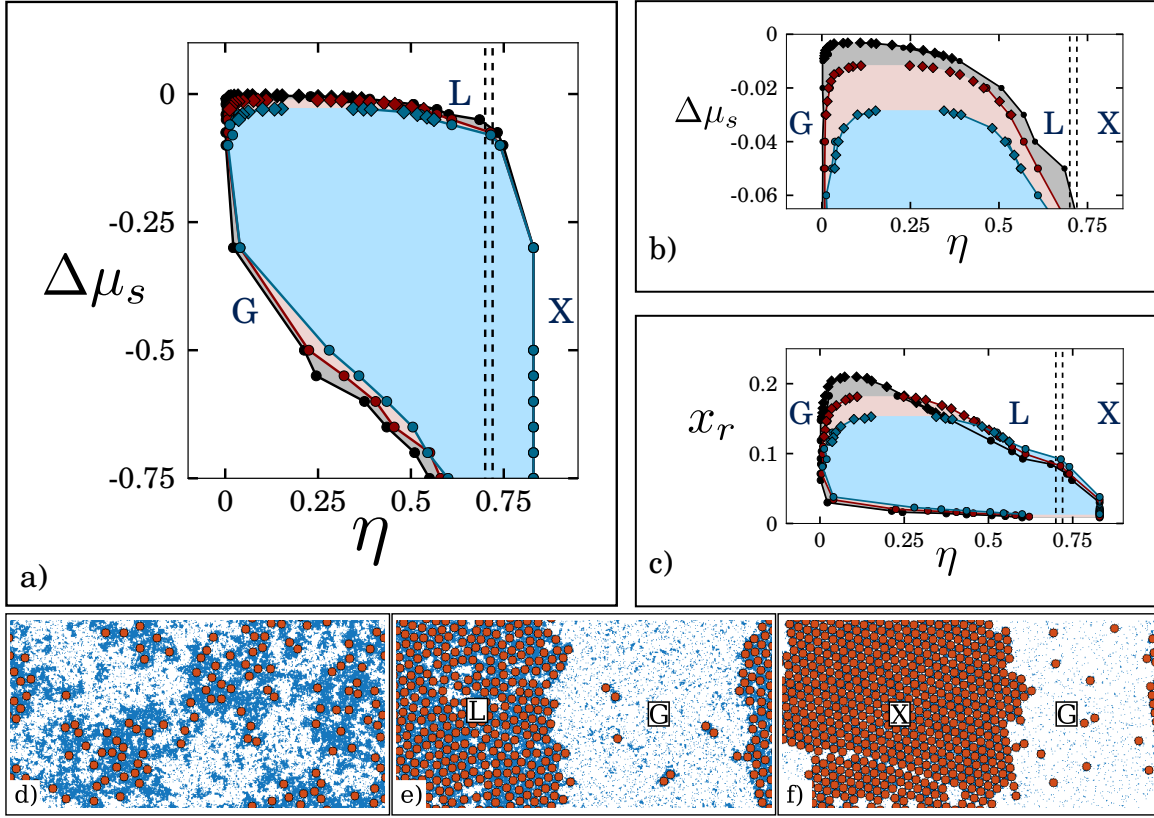


FIG. 3. **Phase diagrams and typical snapshots** : a) Phase diagrams of the full ABC ternary mixture plotted as solvent chemical potential  $\Delta\mu_s$  vs hard disc (colloid) packing fraction  $\eta$  for  $R = 6$ . b) The top portion of a) is replotted for clarity. c) Phase diagram of the ABC model plotted as reservoir solvent composition  $x_r$  vs  $\eta$ . Black, red and blue symbols refer to  $\tau = 0.025$ , 0.05 and 0.075. The diamonds and dots denote the phase boundaries obtained from grand canonical staged insertion Monte Carlo (MC) simulations and  $(\eta, \tau, \Delta\mu_s)$  - ensemble MC simulations, respectively (see Methods). The vertical dashed lines denote fluid-solid coexistence for pure hard discs. d - f) Simulation snapshots of a system of  $256 \times 512$  lattice sites at  $\tau = 0.05$  and  $\alpha = 0.6$ , showing d) a supercritical colloidal phase at  $\Delta\mu_s = -0.005$  of 128 colloids, e) gas-liquid (G-L) coexistence at  $\Delta\mu_s = -0.04$  of 348 colloids, and f) gas-crystal (G-X) coexistence at  $\Delta\mu_s = -0.3$  of 580 colloids.

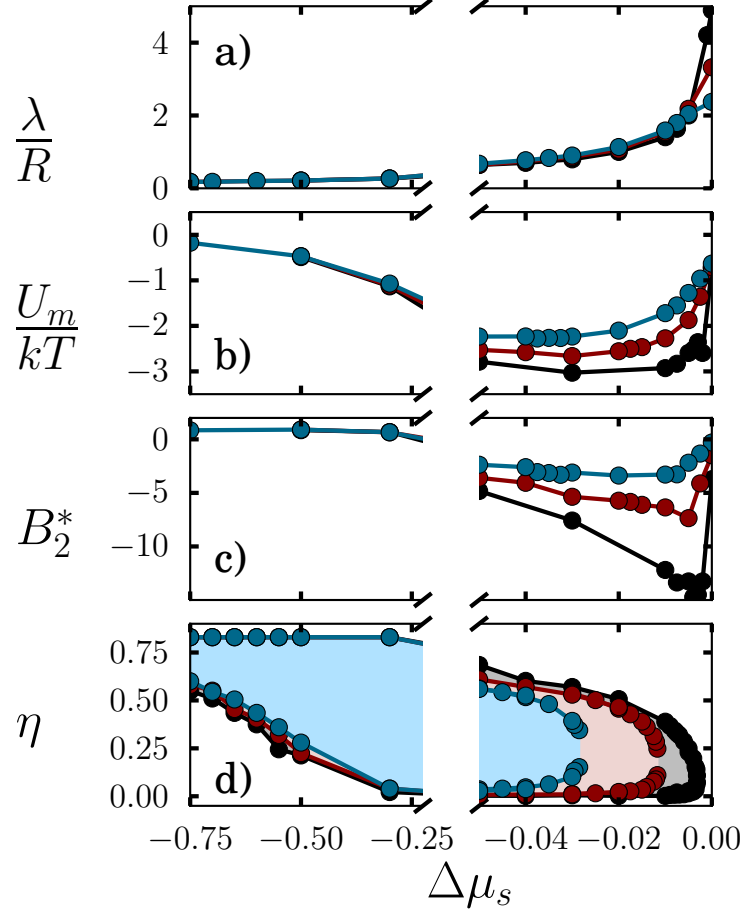


FIG. 4. **Effective two-body SM interactions** a) Thickness  $\lambda$  of the B-rich film adsorbed on a single hard disc, b) The minimum well depth of the effective two-body SM potential, c) The reduced second virial coefficient  $B_2^*$ , d) The phase boundaries of the ternary ABC mixture plotted as hard disc packing fraction  $\eta$  vs  $\Delta\mu_s$ . Black, red and blue symbols refer to reduced temperatures  $\tau = 0.025, 0.05$  and  $0.075$  respectively ( $R = 6, \alpha = 0.6$ ).

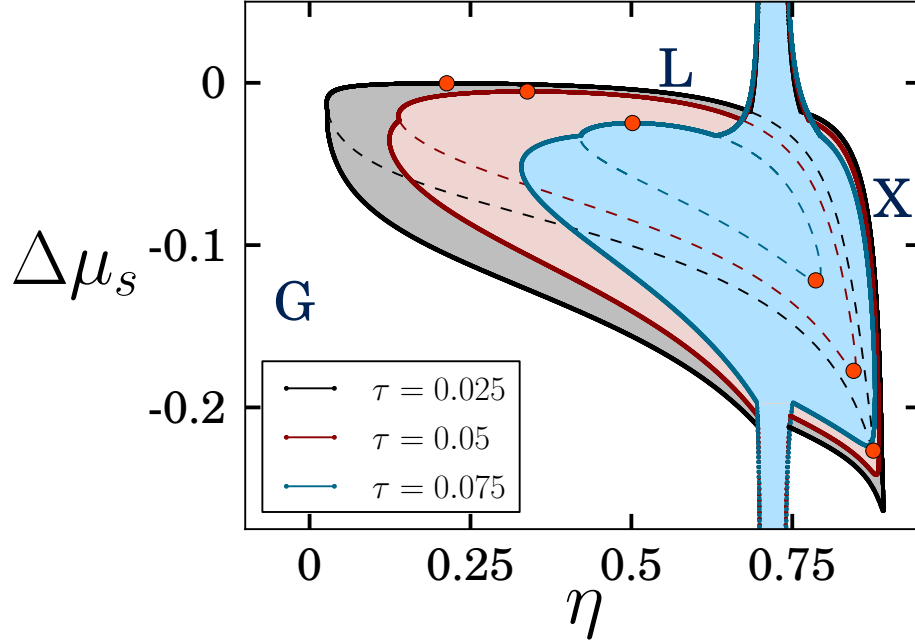


FIG. 5. **Mean-Field predictions for the Phase diagrams:** Binodals (full lines) of the colloid solvent system as calculated within the mean field theory (eqn. 2) for the reduced temperatures  $\tau = 0.025$  (black),  $\tau = 0.05$  (red), and  $\tau = 0.075$  (blue). For each  $\tau$  the upper and lower (G-L) critical points are indicated by the orange dots. Note the 'cusps' in the bottom right corner correspond to iso-structural solid-solid coexistence. The dashed lines correspond to metastable colloidal gas-liquid coexistence. A three-dimensional  $(\tau, \Delta\mu_s, \eta)$  representation of this figure is shown in Fig.S1 of the SI.